International Forum on Aeroelasticity and Structural Dynamics
IFASD 2024
17-21 June 2024, The Hague, The Netherlands

INFLUENCE OF BLADE ELASTICITY AND THRUST ON THE WHIRL FLUTTER STABILITY OF A PROPELLER-DRIVEN AIRCRAFT

Julia Noël[1], Christopher Koch[2], Bernd Stickan[1], Hans M. Bleecke[1], Jürgen Arnold[2]

[1]AIRBUS Operations
Airbus-Allee 1, 28199 Bremen, Germany
julia.noel@airbus.com
bernd.b.stickan@airbus.com
hans.bleecke@airbus.com

[2]Institute of Aeroelasticity, German Aerospace Center (DLR)
Bunsenstraße 10, 37073 Göttingen, Germany
christopher.koch@dlr.de
juergen.arnold@dlr.de

Keywords: Aeroelasticity, Flutter, Whirl Flutter, Propeller, Turboprop

Abstract: Whirl flutter stability is an important certification criterion for propeller-driven aircraft. Recent studies, e.g., with the Transfer-Matrix (TM-) method, have shown a significant stabilization of propeller whirl flutter due to blade elasticity. However, the results have been shown only for simplified dynamic models and the TM-method has not been used on full-aircraft level yet. The work related to this paper provides additions to the TM-method in order to make it useful for practical applications on full-aircraft level, as well as additional insights into the effect of blade elasticity on the whirl flutter behavior of a generic turboprop aircraft model. For the theoretical part, transformations for the propeller transfer matrices are introduced to ensure compatibility in the mass model, unit and coordinate system between the propeller and aircraft model. Furthermore, the transfer matrices are interpolated in airspeed to reduce computational time. As a use case, a generic turboprop aircraft model is introduced and frequency-domain whirl flutter results with rigid and elastic blades as well as varying thrust setting are presented. Results show that the stabilizing influence of blade elasticity observed on simpler models also applies to the full-aircraft model and is stronger than, e.g., the influence of thrust.

1 INTRODUCTION

During the design of propeller aircraft, especially in the layout and structural design of the engine support, whirl flutter prediction plays an important role in ensuring aeroelastic stability [1]. Whirl flutter is an aeroelastic instability of the whirl modes of an elastically supported propeller engine [2]. The whirl modes emerge from the structural engine pitch and yaw modes due to propeller and engine gyroscopic moments, which couple the mode families [3]. The backward whirl mode, in which the whirling motion is oscillating against the shaft rotation, can become unstable due to motion-induced aerodynamic forces on the propeller [2]. Houbolt and Reed [4] developed a commonly used method[1] for predicting these motion-induced aerodynamic forces based on rigid blades and a linearized strip theory for the blade aerodynamics. Rodden and

[1]From now on called Houbolt/Reed method or HR-method in this paper.

Rose [5] used the theoretical method introduced by Houbolt and Reed and demonstrated its application in the context of aircraft flutter analysis with MSC Nastran, laying the basis for the introduction of motion-induced propeller forces into the frequency-domain flutter assessment of full-aircraft configurations. They also introduced simple correction methods for taking the propeller wake effects on the wing aerodynamics into account which are also applied in this work (see section 3.3). The method found extensive application, e.g., for parameter studies [6–8] and is also used for certification analysis [9].

However, one of the main assumptions of the Houbolt/Reed method is the limitation to rigid propeller blades. Although it greatly simplifies the mathematical framework to neglect blade elasticity, its inclusion into whirl flutter analysis has been shown to have a stabilizing impact on whirl flutter. As flexible blades are even more important when studying the aeroelastic stability of tilt-rotor aircraft compared to turboprops, even early publications [10–12] on tilt-rotor whirl flutter include simplified models for modelling blade degree of freedom (DOF). Johnstons results [11] show that including different DOF (e.g., flap or lead-lag motion) can even change the instability mechanism from classical backward whirl flutter towards direct coupling between the blade modes and the nacelle. Moderate amounts of flexibility, as it appears, e.g., in turboprop propellers with clamped blades, has been shown to be purely stabilizing on propeller whirl flutter [13, 14]. Donham [13] pointed out, that it is the dynamic response of the elastic blades to the harmonic excitation in the rotating frame (whirl frequency plus rotational speed) that alters the transfer function between propeller hub motion and hub loads and therefore influences whirl flutter stability. Hoover and Shen [14] included elastic blades into their study of the whirl flutter characteristics of the NASA X-57 aircraft and compared the results to a rigid-blade analysis, also finding a stabilizing influence while including blade elasticity. Their analysis is based on time-domain stability analysis of a coupled multi-body simulation (MBS) model in Dymore [14].

Recent results regarding the influence of blade elasticity [15] have been obtained using the Transfer-Matrix (TM) method in the frequency domain. The TM-method identifies frequency-domain transfer functions from propeller hub motion to hub loads from a time-domain isolated propeller model [16]. The stabilizing effect of including blade elasticity has been demonstrated on a simplified propeller-pylon system and explained by uncovering the underlying mechanism that changes the hub-load transfer functions when considering blade flexibility. The main stabilizing factor is the reduction in the coupling moment between pitch and yaw DOF, $M_{z\theta}$ and $M_{y\psi}$, respectively. This part of the propeller transfer function acts in the direction of the backward whirl mode and drives the instability. The reduction in amplitude of this coupling term has been traced back to inertial forces due to blade deformation (driven by the blade stiffness) as well as an azimuthal shift in the aerodynamic loads due to blade oscillations (driven by the first blade eigenfrequency) [15]. However, the analysis is only conducted for a simplified pylon model with one pitch and yaw DOF each. The question arising from this study is whether this effect is also present in full-aircraft configurations, where, e.g., aerodynamic damping from the wing aerodynamics also plays a role. To answer this question in this paper, the TM-method is applied to add different propeller transfer functions to the aeroelastic model of a generic turboprop aircraft. The current formulation of the TM-method is computationally expensive for such configurations though, as the transfer matrices for the propeller have to be identified for each operating point separately. Furthermore, it requires changes in the dynamic model of the aircraft in order to ensure compatibility of the coordinate system and avoid accounting twice for the propeller mass. The work presented in this paper is based on the master thesis of the first author [17], where more extensive results and explanations can be found. In parallel, the

influence of propeller aerodynamic modelling has been studied using the same aircraft model by Koch [18].
In the first part of this paper, the theory for whirl flutter analysis in the frequency domain, especially using the TM-method, is reviewed and the additions to the existing method are described which ensure an efficient application in practice. In the second part, the aircraft model is briefly described and whirl flutter results between the Houbolt/Reed method and the TM-method using rigid and elastic blades with varying stiffness are presented. In the last part, the results are summarized, discussed and recommendations for future work are given.

2 METHODS

Whirl flutter is triggered by motion-induced unsteady aerodynamic forces on the propeller. Therefore, the transfer behaviour between hub displacements and hub forces is fundamental for whirl flutter analyses [16]. To perform whirl flutter analyses in the frequency domain, the propeller forces F_{prop} need to be described depending on the Laplace variable s, the hub motion X_{hub} and the operating point defined by the flight velocity V, the propeller revolution Ω and the air density ρ. For small perturbations about a reference state, this transfer function can be linearised concerning the hub motion X_{hub} leading to a frequency-dependant transfer matrix $\underline{H}_{prop}$ that describes the linear transfer behaviour of the propeller [16], as shown in Eq. 1.

$$F_{prop} = \underline{H}_{prop}(s, V, \Omega, \rho)\Delta X_{hub} \tag{1}$$

The matrix $\underline{H}_{prop}$ depends on the Laplace variable s and the operating point and also contains the gyroscopic moments. Transforming the hub coordinates X_{hub} to modal coordinates q_h using the propeller mode shapes $\underline{\Phi}_{prop}$ and inserting the term into the aeroelastic equation of motion in modal coordinates leads to:

$$\underline{M}_{gen}\ddot{q}_h + \underline{K}_{gen}q_h = \left[\frac{\rho}{2}V^2\underline{Q}_{gen}(s) + \underline{\Phi}_{prop}^T\underline{H}_{prop}(s, V, \Omega, \rho)\underline{\Phi}_{prop}\right] q_h \tag{2}$$

where $\underline{M}_{gen}$ and $\underline{K}_{gen}$ are the generalised mass and stiffness matrices of the structure and $\underline{Q}_{gen}$ the generalised aerodynamic force matrices (including unsteady aerodynamics from other aircraft components) [16]. Eq. 2 can be solved for its eigenvalues, e.g., by means of the g-method [19], resulting in the frequency and damping values of the aircraft eigenmodes. The damping values can be interpreted for stability assessment of the aircraft and also contain potential whirl flutter instabilities.

There are different methods to determine the matrix $\underline{H}_{prop}$. The first method used in this work is the classical Houbolt/Reed method [4,5] which is used as a reference for the second method, the Transfer-Matrix method [16], which is further developed in this work and applied to perform parameter studies on a generic full-aircraft configuration.

2.1 Houbolt/Reed method

The theory of Houbolt and Reed, as it has been applied in [6] and [16], uses stiffness and damping terms to determine the propeller forces and moments and build the linear description of F_{prop} as in Eq. 1:

$$F_{prop} = \underbrace{\left[\underline{K}_{prop}(V, \Omega) + s\underline{D}_{prop}(V, \Omega) - s\underline{G}(\Omega)\right]}_{\underline{H}_{prop}} \Delta X_{hub} \tag{3}$$

Forces and moments around the propeller axis are neglected in this method, causing the propeller matrices to become 4x4-matrices and the vector of perturbations ΔX_{hub} to consist only

of the displacements in the propeller plane (translation in y and z direction and rotation θ and ψ around these axes). The matrix $\underline{G}$ (compare Eq. 4) describes the gyroscopic matrix containing $M_{gyro} = I_p\Omega$ [3]:

$$\underline{G} = \begin{bmatrix} 0 & 0 & 0 & 0 \\ 0 & 0 & 0 & 0 \\ 0 & 0 & 0 & M_{gyro} \\ 0 & 0 & -M_{gyro} & 0 \end{bmatrix} \tag{4}$$

The stiffness and damping matrices are composed of non-dimensional derivatives as follows [16]:

$$\underline{K}_{prop} = 2\pi qR^3 \begin{bmatrix} 0 & 0 & \frac{C_{y\theta}}{2R} & \frac{C_{y\psi}}{2R} \\ 0 & 0 & \frac{C_{z\theta}}{2R} & \frac{C_{z\psi}}{2R} \\ 0 & 0 & C_{m\theta} & C_{m\psi} \\ 0 & 0 & C_{n\theta} & C_{n\psi} \end{bmatrix}, \underline{D}_{prop} = 2\pi qR^3 \begin{bmatrix} -\frac{C_{y\psi}}{2RV} & \frac{C_{y\theta}}{2RV} & \frac{C_{yq}}{2V} & \frac{C_{yr}}{2V} \\ -\frac{C_{z\psi}}{2RV} & \frac{C_{z\theta}}{2RV} & \frac{C_{zq}}{2V} & \frac{C_{zr}}{2V} \\ -\frac{C_{m\psi}}{V} & \frac{C_{m\theta}}{V} & \frac{C_{mq}R}{V} & \frac{C_{mr}R}{V} \\ -\frac{C_{n\psi}}{V} & \frac{C_{n\theta}}{V} & \frac{C_{nq}R}{V} & \frac{C_{nr}R}{V} \end{bmatrix} \tag{5}$$

with the flight velocity V and the propeller radius R. The first index of the derivatives specifies the resulting force or moment and the second index specifies the deflected degree of freedom that causes this load component. The derivation is based on a linear strip theory approach, only including unsteady aerodynamic effects afterwards via a local Theodorsen function correction [4]. Further, to allow an analytical derivation, the propeller blades are assumed to be rigid and no steady state influence and no induced flow is considered [4].

2.2 Transfer-Matrix method

The Transfer-Matrix method (shortly "TM-method") has been developed to find a method for propeller whirl flutter evaluations in the frequency domain that overcomes some of the limitations mentioned for the HR-method [16]. In this method, the matrix $\underline{H}_{prop}$ is determined directly as a frequency-dependent transfer function between propeller hub motions and forces respectively moments without making use of damping and stiffness matrices, in the form of:

$$F_{prop} = \underbrace{\begin{bmatrix} F_{xx} & F_{xy} & F_{xz} & F_{x\phi} & F_{x\theta} & F_{x\psi} \\ F_{yx} & F_{yy} & F_{yz} & F_{y\phi} & F_{y\theta} & F_{y\psi} \\ F_{zx} & F_{zy} & F_{zz} & F_{z\phi} & F_{z\theta} & F_{z\psi} \\ M_{xx} & M_{xy} & M_{xz} & M_{x\phi} & M_{x\theta} & M_{x\psi} \\ M_{yx} & M_{yy} & M_{yz} & M_{y\phi} & M_{y\theta} & M_{y\psi} \\ M_{zx} & M_{zy} & M_{zz} & M_{z\phi} & M_{z\theta} & M_{z\psi} \end{bmatrix}}_{\underline{H}_{prop}} \Delta X_{hub} \tag{6}$$

where the entries F_{ij} or M_{ij} in the matrix stand for a scalar depending on the frequency defining the force or moment response regarding the i-axis to a perturbation in j direction [16]. The perturbation vector ΔX_{hub} now consists of all six degrees of freedom of the propeller hub. Gyroscopic moments can be included in $\underline{H}_{prop}$ or added to the equation of motion separately as an additional gyroscopic matrix $\underline{G}$. $\underline{H}_{prop}$ is identified using time-domain simulations of an isolated propeller model, which is excited from its steady state for each hub degree of freedom. Simulation tools for this type of time-domain perturbation are already widely spread, having a high fidelity which is carried forward directly into the fidelity of the transfer matrices [16]. In this work, the MBS-tool Simpack [20] is used for modelling the isolated propeller. The perturbation response is then transformed in the frequency domain and provides the transfer functions for the different degrees of freedom and frequencies depending on the perturbation.

As perturbation, a harmonic or pulse excitation can be used. While harmonic excitation can be used also for time-variant conditions (such as non-axial flow), for time-invariant and linear systems, pulse excitation excites a broad spectrum of frequencies in only one time simulation, reducing the computational costs [16]. Each degree of freedom of the propeller hub has to be excited separately to generate the full transfer matrix, whereby however in some cases practical simplifications, e.g. in terms of symmetry, can be made to reduce the computational effort [16].

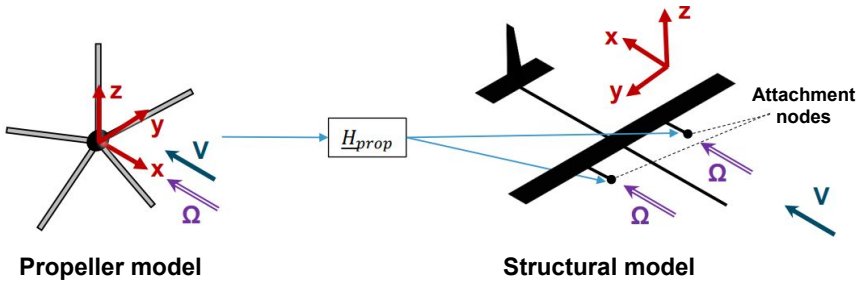

Figure 1: Illustration of the combination of propeller model and structural model

The derived set of transfer matrices is (numerically) coupled with a suitable node of the structural model representing the propeller hub node (see Fig. 1). In past applications of the TM-method, only examinations on a simple two-degree-of-freedom propeller model have been conducted. In these cases the models used have been intentionally built to apply the method. The transfer matrices could be included in the flutter calculation directly after the previously presented identification procedure. However, if more complex aircraft configurations are evaluated, the current TM-method needs to be extended to overcome some limitations the initial procedure has, allowing its direct and efficient application on these models in practice. There are three main challenges that need to be solved and are treated in greater detail in the next subsections:

- The **influence of the propeller mass** that is included in the propeller model in the multi-body simulation, but usually also in the structural model, must not be accounted for twice.
- The **alignment of the propeller model**, which is used to generate the transfer matrices, **and the structural model**, with which it should be combined (e.g. regarding coordinate system orientations) is required.
- The necessity to generate **transfer matrices for each operational point** that should be evaluated in the flutter analysis can get very time consuming for complex models.

To keep the advantages of the TM-method in terms of independency of propeller model and structural model, it is crucial to make it possible to combine different propeller models with different structural models without adapting the specific models. Therefore, to solve the mentioned issues, additional pre-processing steps are added to the method procedure after the transfer-matrix generation and before introducing the transfer matrices into the flutter equation. With this approach, different structural configurations can be used in the analysis without adapting the dynamic airframe model itself.

2.2.1 Elimination of the mass influences from the transfer matrices

The propeller modelled in Simpack always contains the masses of the propeller blades. These masses can not be eliminated from the MBS-model before the transfer-matrix generation, at least for elastic propeller blades, and therefore always influence the generated transfer matrices. However, the propeller masses are usually also part of the finite element model (FE-model) of the airframe and must not be considered twice. Therefore, the masses need to be either

subtracted from the FE-model or from the generated transfer matrices. To keep the FE-models independent from the method used to include the propeller in the flutter analysis, the second option, removing the mass influence from the transfer matrices, is the more practical solution and is realized in the following. Mass has a quadratic influence with increasing frequency in the flutter equation. This is transferable to the mass part in the transfer-matrix term $\underline{H}_{prop}$. Because it is included in the flutter equation on the right side of the equation, the term has a negative sign. The mass from the propeller blades is known from the Simpack model as a mass matrix $\underline{M}_{prop}$ referenced about the propeller hub point. Therefore, with the simplification of $\sigma = 0$ and so $s = i\omega$, the mass part in the transfer matrices can be calculated as:

$$-\underline{M}_{prop}\, s^2 = -\underline{M}_{prop}(i\omega)^2 = \underline{M}_{prop}\, \omega^2 \tag{7}$$

This term can then be subtracted from the generated transfer matrix:

$$\underline{H}_{prop,new} = \underline{H}_{prop} - \underline{M}_{prop}\, \omega^2 \tag{8}$$

with the simplified propeller mass matrix $\underline{M}_{prop}$:

$$\underline{M}_{prop} = \begin{bmatrix} m_{prop} & 0 & 0 & 0 & 0 & 0 \\ 0 & m_{prop} & 0 & 0 & 0 & 0 \\ 0 & 0 & m_{prop} & 0 & 0 & 0 \\ 0 & 0 & 0 & I_p & 0 & 0 \\ 0 & 0 & 0 & 0 & I_\theta & 0 \\ 0 & 0 & 0 & 0 & 0 & I_\psi \end{bmatrix} \tag{9}$$

with the propeller mass m_{prop} and the inertia around the main axes I_p, I_θ and I_ψ. Elements beside the main diagonal, that may occur due to differences between centre of gravity and the reference point at the hub, are neglected. The coupling terms therefore remain in $\underline{H}_{prop,new}$ and are correctly accounted for. The new transfer matrix $H_{prop,new}$ can now be combined with a full FE-model without considering the propeller mass twice. The gyroscopic matrix can be eliminated similarly to the propeller mass matrix, in case a separate gyroscopic matrix shall be included.

2.2.2 Alignment of the transfer matrices with the structural model

The transfer matrices generated by the Simpack model are directly introduced into the flutter equation in relation to the attachment nodes in the structural model as illustrated in Fig. 1. No normalisation or non-dimensionalisation is performed beforehand. As the transfer matrices remain with dimensions, this can cause incompatibilities in case of different unit systems or coordinate systems between propeller and airframe model. In the presented case in Fig. 1, differences in terms of the coordinate system definition of both models, as well as in the unit system are present. Before the generated transfer matrices can be introduced in the flutter equation, they need to be aligned to the structural model to eliminate these discrepancies. As shown in Eq. 6, a fully identified transfer matrix consists of elements which each depend on different degrees of freedom, specified by the indices, and need to be adapted accordingly. These adaptions can be brought together in a transformation matrix $\underline{T}$ which is multiplied element-wise with the generated transfer matrices to apply the necessary changes.
For cases with a gyroscopic moment added separately from the transfer matrices, the change of unit system and orientation of the x-axis also affects the definition of this moment. So, it also needs to be aligned accordingly.

Coordinate system orientation

To align the coordinate system orientation of the models seen in Fig. 1, a coordinate system rotation around the z-axis by 180° is needed. The transformation is illustrated in Fig. 2. For

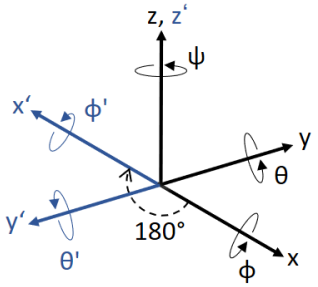

Figure 2: Coordinate system transformation

this rotation a transformation matrix $\underline{T}_{COS}$ is derived, changing the signs of some elements in the transfer matrices by element-wise multiplication:

$$\underline{H}_{prop,cos} = \underline{H}_{prop} \circ \underbrace{\begin{bmatrix} 1 & 1 & -1 & 1 & 1 & -1 \\ 1 & 1 & -1 & 1 & 1 & -1 \\ -1 & -1 & 1 & -1 & -1 & 1 \\ 1 & 1 & -1 & 1 & 1 & -1 \\ 1 & 1 & -1 & 1 & 1 & -1 \\ -1 & -1 & 1 & -1 & -1 & 1 \end{bmatrix}}_{\underline{T}_{COS}} \tag{10}$$

Unit system definition

To adapt the unit system of the propeller model (and of the transfer matrices) to the structural model definition, a transformation matrix $\underline{T}_{unit}$ is derived. The present propeller model uses m as length and kg as mass unit, while the unit system of the structural model uses mm and t, respectively. Dependant on the input and output magnitudes of the single elements of the transfer matrix, different unit conversions are necessary. For the present conversion this leads to the following adaption of the transfer matrices:

$$\underline{H}_{prop/t,mm} = \underline{H}_{prop/kg,m} \circ \underbrace{\begin{bmatrix} 0.001 & 0.001 & 0.001 & 1 & 1 & 1 \\ 0.001 & 0.001 & 0.001 & 1 & 1 & 1 \\ 0.001 & 0.001 & 0.001 & 1 & 1 & 1 \\ 1 & 1 & 1 & 1000 & 1000 & 1000 \\ 1 & 1 & 1 & 1000 & 1000 & 1000 \\ 1 & 1 & 1 & 1000 & 1000 & 1000 \end{bmatrix}}_{\underline{T}_{unit}} \tag{11}$$

2.2.3 Interpolation of the transfer matrices for more velocity steps

For complex models, many operating points, e.g. velocity steps, have to be considered in the flutter analysis to ensure proper mode-tracking and detailed results. For each of these operating points, there needs to be a transfer matrix as input in the flutter analysis. That might make the

TM-generation quite time consuming. To decouple the number of velocity steps used for the TM-generation and those used during the flutter analysis, an interpolation routine is introduced in the procedure to enable the refinement of the velocity steps after the generation of the transfer matrices. For the interpolation routine, a linear method is used that interpolates every TM-value, separately for each base frequency, over the velocity steps. The routine can also extrapolate over the limits of the given velocity steps, but this might lead to wrong results in this range and should be avoided if possible.

3 MODELS

In order to examine the influence of blade elasticity and thrust on full-aircraft level, the flutter stability of a twin-turboprop aircraft with a high-wing configuration and a conventional tail is evaluated. The aircraft has a wingspan of about 16 m and represents a short-distance, short take-off and landing (STOL) commuter aircraft for 20 passengers. Both propellers, mounted each on one wing, rotate in the same direction (clockwise as viewed from the front) with a constant rotational speed of $\Omega = 168.3\ rad/s$. The dive speed V_D of the aircraft is $142\ m/s$.

3.1 Aircraft model

The structural model used for the flutter calculations is a full-span aircraft model for MSC Nastran [21]. The fuselage is modelled using bar elements, while the wing and empennage, as well as the control surfaces, consist of shell elements, which each have a specified material and density. The structural model has been modified to trigger whirl flutter instabilities in the examined velocity range for the flutter analysis with the classical HR-method by reducing the engine mounts stiffness.

To model the unsteady aerodynamics of the aircraft, the commercial aeroelastic software ZAERO [22] is used. The panel model used can be seen in Fig. 3. For the lifting surfaces (empennage and wing), CAERO7 panels are defined while for the other components, BODY7 elements are used. The aerodynamic data is generated with the linear subsonic unsteady aerodynamic ZONA6 method of ZAERO [23].

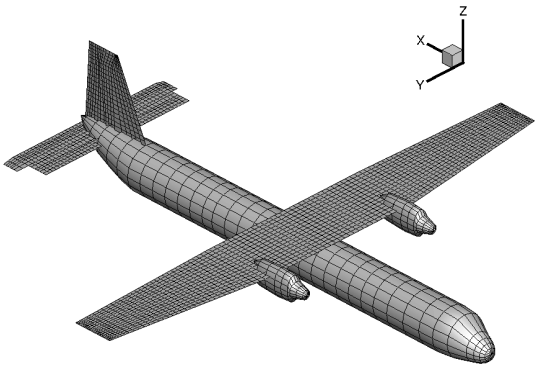

Figure 3: Aircraft aerodynamic model

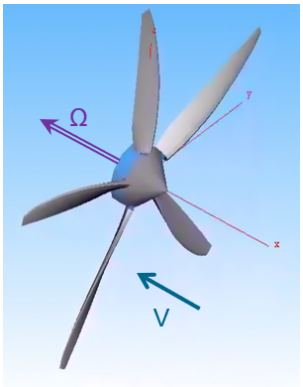

Figure 4: Propeller model in Simpack

3.2 Propeller model

The aircraft is equipped with two identical constant-speed propellers with five propeller blades. For the transfer-matrix generation a propeller MBS-model in Simpack [20] is used. It is the same model as used in reference [15] and is illustrated in Fig. 4. The model includes the propeller blades and the hub, but no further pylon structure. The propeller blades are modelled using linear, finite element beam models. By defining the number of blade modes considered

the propeller blades can be modelled as rigid or elastic (three blade modes are considered for elastic modelling). The model is parametrised, so the blade properties can be adjusted, e.g., to scale the stiffness via a factor k_{scale}. $k_{scale} = 1$ represents the nominal case and higher values leading to a higher blade stiffness. Technical details of the propeller can be found in Table 1.

Table 1: Technical details of the propeller

blade number	N_B	5
rotor diameter	D	$2.5\ m$
blade mass	m_{prop}	$1.542\ kg$
polar blade inertia	$I_{p,blades}$	$3.597\ kgm^2$
additional polar inertia due to engine parts	$I_{p,add}$	$3.093\ kgm^2$
nominal rotational speed	Ω	$168.3\ rad/s$

The propeller aerodynamics are based on an unsteady strip theory approach [24], which is implemented in the Simpack model by means of twelve force elements per blade, each arranged along blade segments in radial direction of the blades. The force elements define the airfoil aerodynamics for each segment with a linear lift slope of $C_{L,\alpha} = 2\pi$, a maximal lift coefficient of $C_{L,max} = 1.5$ and a minimal drag coefficient of $C_{D,min} = 0.15$. The aerodynamic moment is neglected. The flow velocity at each force element is composed of the flight velocity, the propeller rotation, the hub motion and possible blade deformations. Other induced velocities are neglected, as well as influences between the single propeller blade elements. Therefore, especially for high thrust conditions, the aerodynamics are not modelled precisely [15]. For a comparison of the Wagner strip theory with other propeller aerodynamic methods, compare Koch et. al. [25] and a parallel study on full-aircraft level [18]. In the aerodynamic modelling of the propeller, the propeller blades are assumed to have an infinite length. So, no aspect ratio correction is considered. By means of comparability, this is also applied in the HR-method.

Different operating conditions in terms of propeller thrust are examined later on. The propeller is operated as a constant-speed propeller, where the rotational speed is kept constant. The propeller blade pitch angle changes to retain a specific thrust (or power) condition at each operating point [26]. The three trim cases used in this work are described in Table 2. To adjust the propeller to the desired thrust, the collective blade pitch angle is varied iteratively until the corresponding trim target is reached.

Table 2: Trim conditions

case	trim target	comment
windmilling	torque = 0	standard no-thrust case
max. power	power $P_{max} = 500\ kW$	operation with maximal power, ramped up until $0.35\ V_D$ i.o. not to exceed the max. blade AoA
const. T/q	thrust T to dyn. pressure q ratio $T/q = 0.2851\ m^2$	value of "max. power" case at $V = V_D$, used for slipstream correction

3.3 Aerodynamic interaction

To include the influence of the propeller wake on the wing aerodynamics a correction factor accounting for the axial velocity components in the propeller wake is applied for the examinations with thrust. An appropriate factor has been determined by Rodden and Rose [5] and is based on propeller parameters, such as the propeller diameter D and the propeller area S, but also the

operating point. It is defined as follows:

$$w_{kk} = 1 + \frac{D}{\Delta y} \cdot \sqrt{1 + \frac{1}{\sqrt{1 + T/(qS)}}} \cdot \frac{T}{\sqrt{2}qS} \tag{12}$$

It can be remarked that the factor depends on the flight velocity V, but remains constant for a constant ratio of thrust T to dynamic pressure q. Therefore, for the specific trim condition with constant T/q, the factor remains constant over the velocity range. That makes it possible to implement the factor on the aerodynamic pressure coefficients in the flutter calculation using the CPFACT module from ZAERO [22]. Δy labels the width of the area where the factor is applied. The factor is implemented on selected aerodynamic panels (covering the width of the propeller wake) of the ZAERO model of the aircraft. For the present case, the factor sums up to $w_{kk} \approx 1.056$.

4 RESULTS

To examine the flutter stability of the aircraft model, the trends of frequency f and damping g of the structural modes over the flight velocity in a range between 0 and $200\ m/s$ are evaluated.

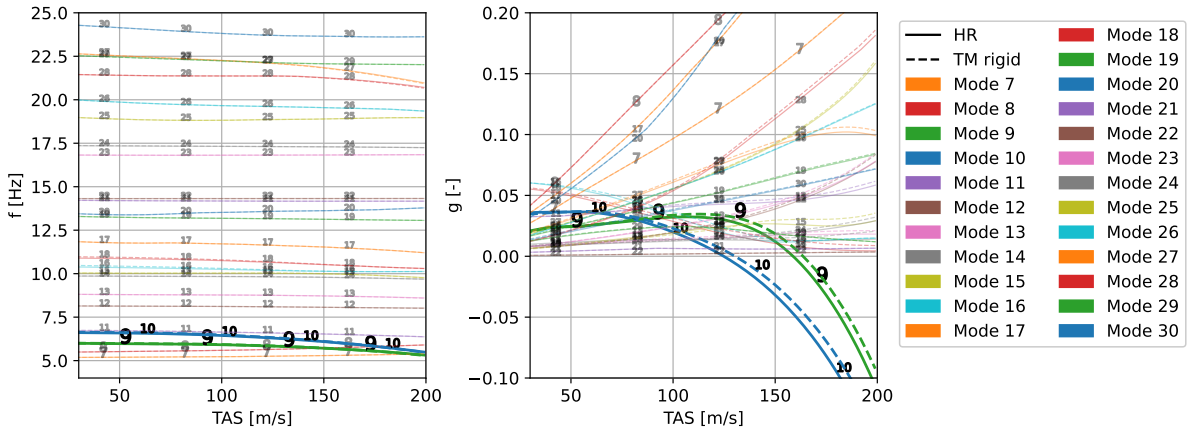

Figure 5: Frequency and damping over the velocity for the structural modes of the aircraft, calculated for rigid propeller blades

For the aircraft model with rigid blade modelling approaches (either via the classical HR-method or the TM-method with rigid propeller blades in Simpack model), two whirl instabilities as seen in Fig. 5 are revealed. The figure shows the trends for the first 30 structural modes, except the rigid body modes, of the aircraft model combined with the HR propeller and the rigid TM propeller. A negative value of g indicates negative damping of a mode and thus, flutter. Two modes can be found that cross the zero-damping line and go unstable. They are highlighted in the plot: Mode 9 and Mode 10. Both instabilities are identified as backward whirl modes. Figs. 6 and 7 illustrate the flutter modes and their whirl direction. For mode 10 (see Fig. 6), the whirl motion of the two propellers occurs in-phase, so both propeller axes are deflected upwards at the same time. In this case, mostly symmetric structural modes with respect to the xz-plane are involved. Still, although both propellers perform a backward whirl motion and the mode is therefore not fully symmetrical, this mode is referred to as ”symmetric whirl” in the following. In the other case, for mode 9 (see Fig. 7), the whirl motion of both propellers occur with a phase offset. When one axis is deflected upwards, the other axis is deflected downwards. Still, both propellers are performing a backward whirl motion, but mostly anti-symmetrical struc-

tural modes are involved in the airframe motion. In the following, this mode is referred to as ”antisymmetric whirl”.

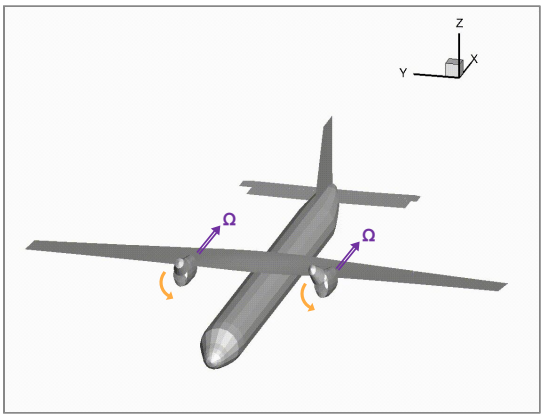

Figure 6: ”Symmetric whirl”

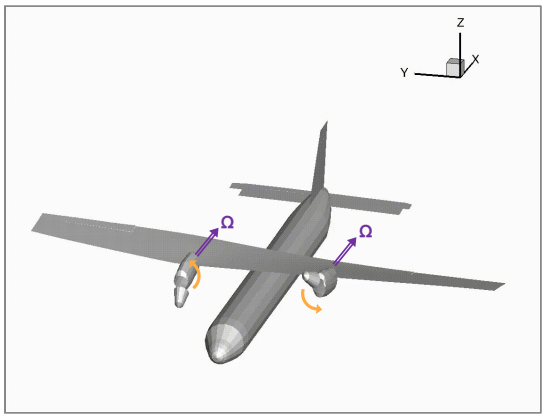

Figure 7: ”Antisymmetric whirl”

Both rigid blade methods show these two instabilities. However, the HR-method results show lower flutter speeds ($124.81\ m/s$ and $158.77\ m/s$) than the TM-method results ($130.32\ m/s$ and $163.64\ m/s$). The difference between HR- and TM-method even for rigid propeller modelling has already been present in analyses of a simple two-degree-of-freedom model (see [15]). Therefore, it is expected to appear also on full-aircraft level and can be explained in this case in the same way by simplifications in the HR-method. As the HR-method results in lower flutter speed, it is still the more conservative method. In the following, the influence of blade elasticity and thrust on both unstable modes is examined.

4.1 Influence of blade elasticity

To examine the influence of blade elasticity, transfer matrices generated with the Simpack model with elastic blades are used for the flutter analysis. Models with different stiffness scales k_{scale} are used to reveal trends in the results. In the following, only the trends for the two unstable modes are displayed. Fig. 8 shows the frequency and damping over the velocity for these two modes for different blade stiffness values, as well as the rigid propeller results from the previous section. Increasing the blade elasticity from rigid to nominal blade stiffness ($k_{scale} = 1$) leads to a higher damping and a stabilising effect for both modes. For relatively stiff blades with $k_{scale} = 10$, the frequency and damping curves are close to the results from the rigid propeller modelling, but indicate higher flutter velocities for both flutter modes. At nominal blade stiffness, no instability is present any more in the examined velocity range.

However, when increasing the elasticity further ($k_{scale} < 1$), the damping level decreases again and the system becomes unstable again. Especially, the model with very soft blades ($k_{scale} = 0.25$) shows an early instability for the symmetric whirl mode (mode 11 instead of mode 10 for this case, due to a mode switch). For this case, it needs to be remarked that few other new flutter modes appear on other structural modes (which are not displayed here) and have not been examined further. In general, the results for blades as flexible as this have to be handled with caution because it has to be investigated further how the TM-method depicts these new effects. However, it can be concluded that aircraft configurations with very soft propeller blades need to be handled with care. For detailed knowledge about the arising effects, further studies are necessary.

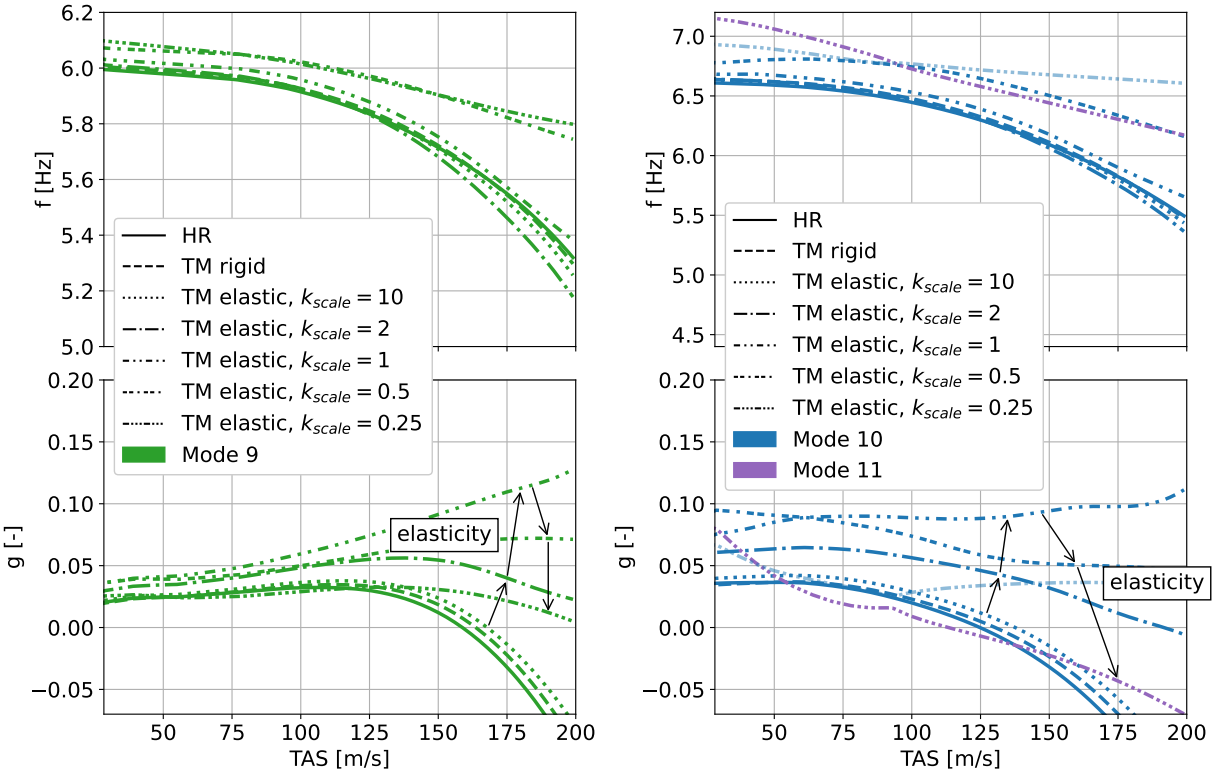

(a) Mode 9 (antisym. whirl)

(b) Mode 10 (sym. whirl)

Figure 8: Influence of blade elasticity on frequency and damping of whirl flutter modes (windmilling condition)

4.2 Influence of thrust

For the examination of the influence of thrust on the whirl flutter stability of the generic aircraft configuration, two trim conditions have been defined: the max. power condition and the const. T/q condition (see Tab. 2). Figure 9 shows the frequency and damping of the two modes that go unstable in the rigid windmilling case (see previous section) for the different trim conditions for a model with rigid propeller blades (a) and a model with elastic propeller blades (b). The results are all generated using the TM-method. For the elastic model with max. power trim, mode 11 is plotted instead of mode 10 due to an occurring mode switch in the results.

With rigid blade modelling, it can be seen that there is no significant influence of the different trim conditions on the frequency as well as the damping. It can be further noticed that this (small) influence of thrust compared to the windmilling case is not clearly stabilising or destabilising for this configuration. Comparing the windmilling condition with the max. power case, the flutter velocity for mode 9 is slightly decreased due to thrust (from $163.64\ m/s$ to $163.32\ m/s$). In contrast to that, for mode 10 the thrust has a slightly stabilising effect. The flutter velocity increases from $130.32\ m/s$ to $131.40\ m/s$ for the max. power case. The difference is a bit higher than for mode 9, but still less than one percent.
For the elastic blade model, a bigger influence on the damping level appears. The damping increases over the full velocity range for both modes due to thrust. For the max. power case, the impact in the lower velocity range is larger than for higher velocities (except for the very low velocities up to approximately $50\ m/s$ where the power is ramped up and not yet on full level). This appearance fits to the trim condition that leads to higher thrust at lower velocities to keep the power constant. For the const. T/q trim condition, the difference compared to the windmilling case is smaller in the lower velocity range and amplifies for higher velocities. This

can be explained by the definition of the trim condition which leads to less thrust for low velocities to keep the thrust to dynamic pressure ratio constant. It needs to be remarked that due to the assumptions made in the g-method, the damping values besides the flutter point are not determined exactly, so the difference in damping should not be interpreted too precisely.

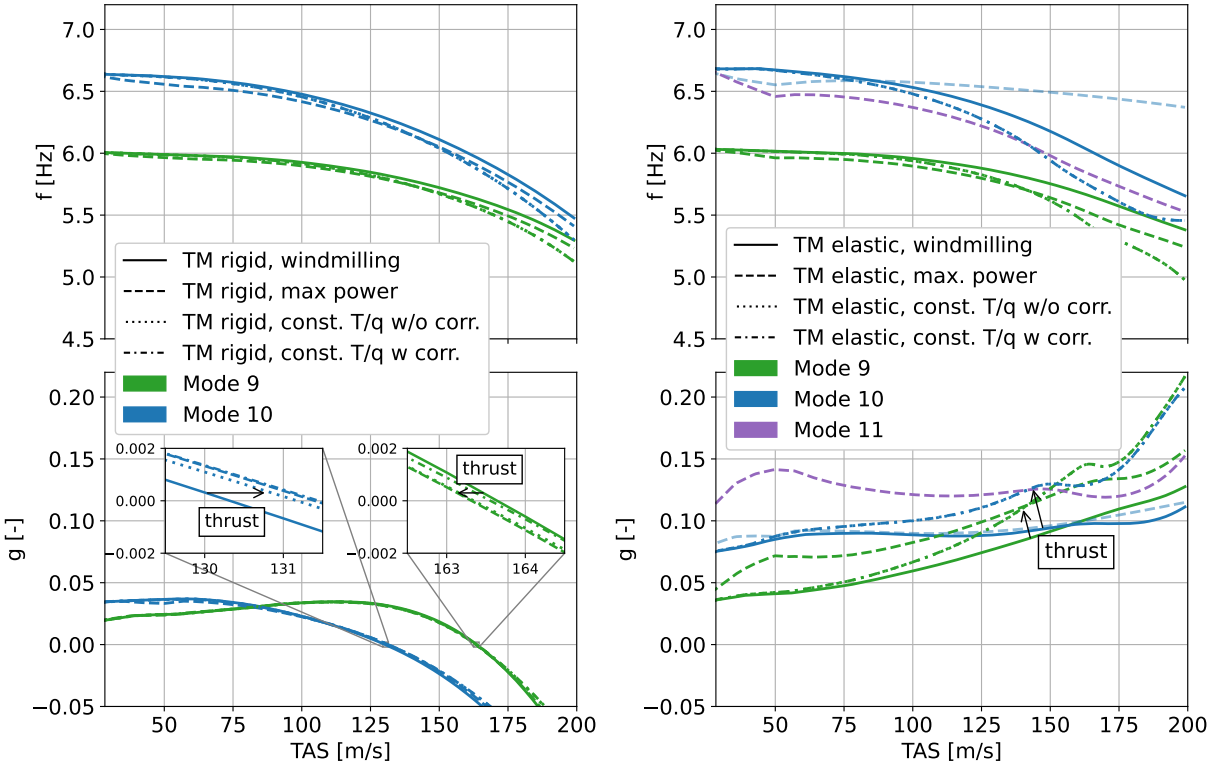

(a) Rigid blades

(b) Elastic blades ($k_{scale} = 1$)

Figure 9: Influence of thrust on frequency and damping of whirl flutter modes

4.3 Influence of a slip stream correction factor

The second trim condition with thrust (const. T/q) has been established to include the correction factor for aerodynamic interactions as presented in section 3.3. For the examined case, this factor ($w_{kk} = 1.056$) is quite small. Therefore, it is expected that its influence on the flutter stability is also small. This hypothesis can be confirmed by looking at the frequency and damping plots displayed in Fig. 9. Comparing only the two cases with const. T/q trim with and without using the slip stream correction factor w_{kk} reveals, that an influence of the factor for rigid and elastic blade modelling is barely existing. Only in the close-up in figure 9 (a) a difference can be observed showing that including the slipstream correction factor leads to slightly higher flutter speeds for both unstable modes. But, the difference is still very small.
The thrust to dynamic pressure ratio used is relatively small. The assumed value for trim has been determined by taking the thrust and pressure value from the reference point at V_D. The effect of the slipstream correction might be larger for T/q values using the maximum thrust at lower velocities. If the reference condition is not determined at V_D, but, for example, at the Design Manoeuvring Speed of $V_A = 72\ m/s$ of the aircraft, the ratio increases to a value of approximately $T/q = 2$. In this case the factor w_{kk} becomes 1.38, which is much higher than the calculated value before. However, the influence of such a factor has not been tested because for whirl flutter usually a higher velocity range is relevant. But, for load analysis this slip stream correction might have a larger impact as those are performed also at lower velocities.

5 CONCLUSION AND OUTLOOK

In the work related to this paper, the Transfer-Matrix method for representing propeller models in a frequency-domain whirl flutter analysis has been improved for practical applications. Additional pre-processing steps are included to ensure compatibility of the transfer matrices with the airframe model in terms of mass model, coordinate and unit system, thus eliminating unnecessary adaptions of the airframe model. Furthermore, interpolation over a range of airspeeds is used to save computational time. In the future, the coordinate transformations could be derived for arbitrary coordinate system angles. Additionally, linear interpolation of the transfer matrices only works in the low-frequency range below the first eigenmodes of the propeller. More complex interpolation schemes have to be used in case the resonance peaks of the blade modes are to be interpolated, too.

The paper presents flutter results for a generic, twin-engine turboprop aircraft model in free flight. The structural configuration is tuned to show two whirl flutter couplings for the classical rigid blade analysis. Moderate levels of blade elasticity have a strong stabilizing effect on the backward whirl modes, eliminating whirl flutter in the airspeed range studied. This confirms results with a simplified pylon model from previous studies. Very flexible blades lead to a destabilization, which can be accounted to additional couplings of the airframe with the propeller blade modes.

Flutter predictions for trim states with thrust and engine power deviate only slightly from those in windmilling, especially for the rigid blade case. The (already positive) damping of the whirl modes in the elastic blade case is further increased. The slipstream correction of the wing aerodynamics has a negligible influence on the flutter instabilities investigated. In this case, the missing velocities induced by the oscillating wing at the propeller hub might have an additional influence on the whirl flutter predictions. These interaction effects should be examined further in future work, e.g., using CFD-methods.

The results shown in this paper regarding the influence of blade elasticity and thrust are obtained with numerical simulation only and should be validated in the future, e.g., using high-fidelity numerical simulations, wind-tunnel experiments or in-flight damping measurements. Additional numerical parameter studies might also reveal more details of the influence of aerodynamic and structural parameters, such as the individual blade stiffnesses in bending and torsion. All of this might increase the confidence in the results presented in this study, in order to exploit them for the design of the next generation of propeller aircraft.

6 REFERENCES

[1] Hrycko, G. (1983). Design of the low vibration turboprop powerplant suspension system for the DASH 7 aircraft. *SAE Transactions*, 92, 133–145. ISSN 0096736X, 25771531.

[2] Reed, W. (1966). Propeller-rotor whirl flutter: A state-of-the-art review. *Journal of Sound and Vibration*, 4(3), 526–544. ISSN 0022460X. doi:10.1016/0022-460X(66)90142-8.

[3] Cecrdle, J. (2015). *Whirl Flutter of Turboprop Aircraft Structures*. Elsevier. ISBN 978-1-78242-185-6. doi:10.1016/B978-1-78242-185-6.50017-9.

[4] Houbolt, J. and Reed III, W. (1962). Propeller-nacelle whirl flutter. *Journal of the Aerospace Sciences*, 29(3), 333–346.

[5] Rodden, W. and Rose, T. (1989). Propeller/nacelle whirl flutter addition to MSC/NASTRAN. In *Proceedings of the 1989 MSC World User's Conference*.

[6] Koch, C. (2021). Parametric whirl flutter study using different modelling approaches. *CEAS Aeronautical Journal*, 13, 57–67. ISSN 1869-5582, 1869-5590. doi:10.1007/s13272-021-00548-0.

[7] Böhnisch, N., Braun, C., Muscarello, V., et al. (2023). A Sensitivity Study on Aeroelastic Instabilities of Slender Wings with a Large Propeller. In *AIAA SCITECH 2023 Forum*. National Harbor, MD & Online: American Institute of Aeronautics and Astronautics. doi:10.2514/6.2023-1893.

[8] Cecrdle, J. (2012). Analysis of Twin Turboprop Aircraft Whirl-Flutter Stability Boundaries. *Journal of Aircraft*, 49(6), 1718–1725. doi:10.2514/1.C031390.

[9] Cecrdle, J. (2019). Whirl flutter-related certification according to FAR/CS 23 and 25 regulation standards. In *International Forum on Aeroelasticity and Structural Dynamics 2019, IFASD 2019*. Savannah, GA (USA).

[10] Young, M. and Lytwyn, R. (1967). The Influence of Blade Flapping Restraint on the Dynamic Stability of Low Disk Loading Propeller-Rotors. *Journal of the American Helicopter Society*, 12(4), 38–54.

[11] Johnston, R. (1972). Parametric Studies of instabilities associated with large, flexible rotor propellers. In *28th Annual National Forum of the American Helicopter Society*. Washington, D.C.: American Helicopter Society.

[12] Johnson, W. (1974). Dynamics of tilting proprotor aircraft in cruise flight. NASA Technical Note NASA TN D-7677, NASA.

[13] Donham, R. E. (2005). Effect of propeller blade bending dynamics on 1P loads and whirl flutter. In *Proceedings of International Forum on Aeroelasticity and Structural Dynamics (IFASD)*, vol. 28. München.

[14] Hoover, C. B. and Shen, J. (2019). Fundamental understanding of propeller whirl flutter through multibody dynamics. In *AIAA Scitech 2019 Forum*. San Diego, California: American Institute of Aeronautics and Astronautics. doi:10.2514/6.2019-1864.

[15] Koch, C. and Koert, B. (2023). Including Blade Elasticity into Frequency-Domain Propeller Whirl Flutter Analysis. *Journal of Aircraft*, 1–11. doi:10.2514/1.C037501.

[16] Koch, C. (2022). WHIRL FLUTTER STABILITY ASSESSMENT USING ROTOR TRANSFER MATRICES. In *International Forum on Aeroelasticity and Structural Dynamics (IFASD) 2022*. Madrid, Spain.

[17] Noël, J. (2023). Influence of more accurate propeller modelling on the whirl flutter stability of a propeller-driven aircraft. Master thesis, DLR-IB-AE-GO-2023-162, https://elib.dlr.de/201017/.

[18] Koch, C. (2024). Whirl flutter analysis using linearized propeller transfer matrices. In *International Forum on Aeroelasticity and Structural Dynamics (IFASD) 2024*. Den Haag, NL. Unpublished.

[19] Chen, P. C. (2000). Damping Perturbation Method for Flutter Solution: The g-Method. *AIAA Journal*, 38(9), 1519–1524. ISSN 0001-1452, 1533-385X. doi:10.2514/2.1171.

[20] Dassault Systemes (2023). *SIMULIA Simpack 2023 Refresh 2*. https://www.3ds.com/de/produkte-und-services/simulia/produkte/simpack.

[21] Hexagon AB (2022). MSC Nastran 2022.3 Quick Reference Guide.

[22] ZONA Technology Inc. (2020). *ZAERO User's Manual, Version 9.3*. https://www.zonatech.com/Documentation/ZAERO_9.3_Users_Full_Electronic.pdf.

[23] ZONA Technology Inc. (2020). *ZAERO Theoretical Manual, Version 9.3*. https://www.zonatech.com/Documentation/ZAERO%209.3_THEO_Full_Electronic.pdf.

[24] Arnold, J. and Waitz, S. (2018). Using Multibody Dynamics for the Stability Assessment of a New Double-Swept Rotor Blade Setup. In *ERF 2018 - 44th European Rotorcraft Forum*. Delft, The Netherlands.

[25] Koch, C., Böhnisch, N., Verdonck, H., et al. (2024). Comparison of Unsteady Low- and Mid-Fidelity Propeller Aerodynamic Methods for Whirl Flutter Applications. *Applied Sciences*, 14(2). doi:10.3390/app14020850.

[26] Hitchens, F. (2015). *Propeller Aerodynamics : The History, Aerodynamics & Operation of Aircraft Propellers*. Andrews UK Ltd. ISBN 9781785381249.

COPYRIGHT STATEMENT